Locus coeruleus MRI contrast is associated with cortical thickness in older adults

Shelby L. Bachman[1,2*], Martin J. Dahl[3], Markus Werkle-Bergner[3], Sandra Düzel[3], Caroline Garcia Forlim[4], Ulman Lindenberger[3,5], Simone Kühn[4,6], & Mara Mather[1*]

[1]Davis School of Gerontology, University of Southern California, Los Angeles, CA, USA
[2]Berlin School of Mind and Brain, Humboldt Universität zu Berlin, Berlin, Germany
[3]Center for Lifespan Psychology, Max Planck Institute for Human Development, Berlin, Germany
[4]Department of Psychiatry and Psychotherapy, University Clinic Hamburg-Eppendorf, Hamburg, Germany
[5]Max Planck UCL Centre for Computational Psychiatry and Ageing Research, London, UK & Berlin, Germany
[6]Lise Meitner Group for Environmental Neuroscience, Max Planck Institute for Human Development, Berlin, Germany

*Correspondence should be addressed to SLB (sbachman@usc.edu) and MM (mara.mather@usc.edu)

Abstract

There is growing evidence that integrity of the locus coeruleus - norepinephrine (LC-NE) system is important for later-life cognition. Less understood is how LC-NE system integrity relates to brain correlates of cognition, such as brain structure. Here, we assessed the relationship between cortical thickness and a measure of LC neuronal integrity in older (n = 229) and younger adults (n = 67). Using neuromelanin-sensitive MRI, we assessed LC integrity as a contrast between signal intensity of the LC and that of neighboring pontine reference tissue. The Freesurfer software suite was used to quantify cortical thickness. We found that LC contrast was positively related to cortical thickness in older but not younger adults, and this association was prominent in parietal, frontal, and occipital regions. Brain regions where LC contrast was related to cortical thickness include portions of the frontoparietal network and have been implicated in cognitive functions which are subject to strong noradrenergic modulation. These findings provide novel evidence for a link between LC integrity and brain structure in later adulthood.

Keywords:

Aging, brain structure, cortical thickness, frontoparietal network, locus coeruleus, norepinephine

Abbreviations: BASE-II = Berlin Aging Study-II, LC = locus coeruleus, DPT = dorsal pontine tegmentum, FPN = frontoparietal network, MMSE = Mini Mental State Examination, MRI = magnetic resonance imaging, NE = norepinephrine, NM = neuromelanin

1. Introduction

A central goal of aging research is to identify factors that protect against aspects of age-related decline. Recently, the locus coeruleus-norepinephrine (LC-NE) system has been postulated as one such factor shaping later-life cognition (Mather & Harley, 2016; Robertson, 2013; Weinshenker, 2018). NE, a neurotransmitter released during arousal, facilitates neural and cognitive processes involved in vigilance, attention and memory (Sara, 2009). The brain's primary source of NE is the LC, a brainstem nucleus located adjacent to the lateral floor of the fourth ventricle (Sara & Bouret, 2012). The LC is densely packed with neurons that release NE throughout the brain (Schwarz & Luo, 2015); through these distributed projections, the LC stimulates neural responses that promote processing of relevant or salient information (Berridge & Waterhouse, 2003; Mather et al., 2016).

A longitudinal study of 165 older adults provided initial evidence that integrity of the LC relates to cognitive performance in aging (Wilson et al., 2013). Post mortem brain autopsies revealed that LC neuronal density was higher in individuals who had exhibited slower cognitive decline over a 6-year period before death, even after controlling for the presence of neurofibrillary tangles and Lewy bodies in the brainstem and neocortical regions.

Studying the LC in vivo in humans has historically been challenging due to the small size of this nucleus. In recent years, however, the human LC has been imaged using magnetic resonance imaging (MRI) sequences that are sensitive to neuromelanin (NM) (Betts et al., 2019b; Liu et al., 2017; Sasaki et al., 2006). NM is a pigment byproduct of catecholamine metabolism and accumulates in aminergic nuclei including the LC (Fedorow et al., 2005; Mann & Yates, 1974). Due to NM's paramagnetic (T1-shortening) properties, these "NM-sensitive" MRI sequences permit NM-containing nuclei – such as the LC – to be identified as hyperintense regions distinguishable from surrounding tissue (Keren et al., 2009; Shibata et al., 2006; Trujillo et al., 2017). Although the contrast mechanisms in NM-sensitive sequences remain to be fully understood (Watanabe et al., 2019a; Watanabe et al., 2019b), signal intensity contrast between the LC and surrounding pontine tissue in NM-sensitive scans (henceforth referred to as LC

contrast) has been validated through histological analysis, with locations of high LC contrast corresponding to the locations of NM-containing cells within the LC (Keren et al., 2015).

Studies using LC contrast derived from NM-sensitive MRI have pointed to the importance of the LC-NE system in cognitive aging: in one study, LC contrast was positively related to cognitive reserve (Clewett et al., 2016), one indicator of the brain's resilience against age-related pathology (Stern, 2009). LC contrast has also been linked to memory ability, with older adults with greater LC contrast having better episodic memory performance (Dahl et al., 2019; Hämmerer et al., 2018). Additionally, individuals with Alzheimer's disease (Betts et al., 2019a) and Parkinson's disease (Liu et al., 2017) exhibited reduced LC contrast compared to healthy older adults. Together, these studies suggest a potentially protective role of LC neuronal integrity, as indexed by LC contrast, in older adulthood.

Of relevance to later-life cognition, NE released from the LC may protect against age-related neuropathology. For example, NE protects against neuroinflammation (Feinstein et al., 2016), regulates microglial functions that facilitate the clearance of amyloid beta (Heneka et al., 2010), contributes to increased expression of neurotrophic factors (Braun et al., 2014), reduces damage from neurotoxicity (Madrigal et al., 2007), and alleviates oxidative stress (Troadec et al., 2001). In addition, NE modulates a host of cognitive processes that typically decline with age, including selective attention (Mather et al., 2016; Sara, 2009), working memory (Berridge & Waterhouse, 2003), memory for emotional events (Strange & Dolan, 2004), and cognitive flexibility (Lapiz & Morilak, 2006). As such, having preserved integrity of the LC-NE system in older adulthood could enhance cognitive outcomes by protecting against brain pathology and by modulating cognitive processes (Mather & Harley, 2016; Robertson, 2013).

If the LC-NE system has a protective role in older adulthood, one prediction is that LC integrity should be associated with cortical integrity. Older adults with relatively well-preserved thickness and volume of the cerebral cortex exhibit better cognitive performance (Nyberg et al., 2012), and reductions in these measures have been shown to explain a large amount of the variance in age-related cognitive decline (Fjell & Walhovd, 2010). For instance, greater frontal and parietal gray matter volumes in older adulthood have been associated with higher cognitive reserve (Bartrés-Faz et al., 2009), and greater

cortical thickness has been linked to better fluid cognitive ability (Fjell et al., 2006). If the LC-NE system protects against age-related neurodegeneration, integrity of this system should be related to brain structure.

To test this possibility, we examined the relationship between an in vivo measure of LC integrity and cortical thickness in older and younger adults. We quantified LC contrast using NM-sensitive MRI and used Freesurfer to assess thickness of the cortical surface. Based on previous evidence supporting a role of the LC in cognitive aging (Dahl et al., 2019; Hämmerer et al., 2018; Wilson et al., 2013), we hypothesized that individuals with higher LC contrast would have greater cortical thickness. Further, we predicted that this association would be strongest in brain regions that are recruited by NE modulated cognitive functions such as attention, cognitive flexibility, and memory (Corbetta et al., 2008; Robertson, 2014; Sara & Bouret, 2012).

2. Methods

2.1. Participants

Data were collected as part of the Berlin Aging Study II (BASE-II), a longitudinal study which aimed to characterize cognitive, neurobiological, social, and physiological factors that contribute to successful aging (Bertram et al., 2014; https://www.base2.mpg.de). NM-sensitive imaging was only performed during the study's second MR measurement-timepoint on a MR-eligible subsample of the BASE-II cohort. Accordingly, those participants who underwent neuroimaging at the second timepoint were selected for this study (n = 323). These individuals were older and younger adults with no history of neurological disorder, psychiatric disorder, or head injury. All participants were right-handed with normal or corrected-to-normal vision. Data for eligible participants were acquired between December 2015 and June 2016 at the Max Planck Institute for Human Development in Berlin, Germany. The Ethics Committees of the German Psychological Society and of the Max Planck Institute for Human Development approved the MRI procedure. All participants provided written, informed consent prior to participation.

Participants were excluded if they did not have complete neural (n = 19) or demographic (n = 1) data. Following visual inspection of NM-sensitive MR scans, additional participants were excluded due to incorrect scan positioning (n = 3), motion artefact (n = 2), or incorrect placement of the LC search space (n = 1; see Section 2.3). One additional participant was excluded for having an inadequate cortical reconstruction. The final sample, which is described in Table 1, consisted of 229 older adults (82 females) with a mean age of 72.3 years (*SD* = 4.10, range = 63-83) and 67 younger adults (22 females) with a mean age of 32.6 years (*SD* = 3.62, range = 25-40). Older and younger adults did not differ significantly in terms of gender distribution, $\chi^2(1, 296) = 0.0917$, $p = 0.762$, or mean years of education, $t(104.4) = -0.347$, $p = 0.729$. The older adult cohort had a significantly higher mean body mass index than did the younger adults, $t(82.3) = 6.83$, $p < .001$. Mini Mental State Examination (MMSE) scores for the older adult cohort ranged from 22 to 30. No exclusions were performed based on MMSE scores.[1] The final sample constituted a 99% overlap with the sample of BASE-II analyzed by Dahl et al. (2019).

Table 1

Sample characteristics

	Younger adults (*n* = 67; 22 females)				Older adults (*n* = 229; 82 females)			
	Mean	SD	Min	Max	Mean	SD	Min	Max
Age	32.6	3.62	25	40	72.3	4.10	63	83
BMI	23.0	3.75	11.6	31.9	26.7	3.49	19.1	37.9
Education	14.3	2.54	10	18	14.1	2.94	7	18
MMSE	-	-	-	-	28.6	1.30	22	30

Note. Age and education are expressed in years. BMI = body mass index; MMSE = Mini Mental State Examination; SD = standard deviation.

[1]Excluding the two older adult participants who scored less than 24 on the MMSE did not change the pattern of results.

2.2. MRI Data Acquisition

MRI data were acquired using a 3-Tesla Siemens Magnetom Trio scanner with a 12-channel head coil. Only sequences used for the present analyses are described in this section.

A three-dimensional, T1-weighted magnetization prepared rapid acquisition gradient-echo (MPRAGE) MRI sequence was applied in the sagittal plane (TR = 2500 ms, TE = 4.77 ms, TI = 1100 ms, scan flip angle = 7º; bandwidth = 140 Hz/pixel, field of view = 256 mm, number of slices = 192, isometric voxel size = 1 mm^3, echo spacing = 10.9 ms; duration = 9:20 min).

Based on the MPRAGE sequence, a NM-sensitive, high-resolution T1-weighted turbo spin echo sequence was applied by aligning the field of view orthogonally with respect to the anatomic axis of the respective participant's brainstem (TR = 600 ms; TE = 11 ms; flip angle = 120º; bandwidth = 287 Hz/pixel; field of view = 256 mm; voxel size = 0.5 x 0.5 x 2.5 mm^3; echo spacing = 10.9 ms; duration = 2 x 5:54 min). This two-dimensional sequence included ten axial slices and a 20% gap between slices in the z-dimension, thereby encompassing the entire pons. For some participants, fewer slices were acquired due to specific absorption rate limits being exceeded (for details, see Dahl et al., 2019; for a discussion, see Betts et al., 2019b). Four online averages during the sequence were performed, yielding two NM-sensitive scans per participant.

2.3. LC Neuromelanin Signal Intensity Assessment

We obtained LC contrast estimates using a semi-automated method of extracting LC signal intensity values, as described by Dahl et al. (2019). This approach yielded a LC location probability map that corresponded to published LC masks (Betts et al., 2017; Keren et al., 2009; Liu et al., 2019) as well as intensity estimates that corresponded to those determined through manual LC delineation. Using this approach, NM-sensitive scans were aligned and pooled across participants to generate a template brainstem volume (Figure 1A-C). The brainstem template was thresholded based on the signal intensity of a reference region in the neighboring dorsal pontine tegmentum (DPT), yielding a binarized LC search space (Figure 1D, 1E). After verifying that this search space encompassed the LC on a group level, this search space was applied as a mask on individual, template-coregistered brainstem volumes. The intensity

and location of the maximum-intensity voxel within the masked region was extracted for each slice in the z- (rostrocaudal) direction of each masked volume. Likewise, a binarized mask of the DPT reference region was applied to template-coregistered brainstem volumes, and the intensity and location of the maximum-intensity DPT voxel was extracted for each slice. LC contrast values were calculated for each slice as a ratio (Betts et al., 2019b; Sasaki et al., 2006), according to the following formula:

(intensity of peak LC voxel – intensity of peak DPT voxel) / intensity of peak DPT voxel

LC contrast values for each hemisphere were assessed in each participant's two brainstem volumes separately and values were subsequently averaged across volumes. A structural equation model was used to estimate an overall value of LC contrast for each participant by identifying the peak LC contrast value across all MRI dimensions (Dahl et al., 2019); these estimates will henceforth be referred to as overall LC contrast values. In addition, for analyses of contrast along the LC's rostrocaudal axis, we averaged LC contrast values across hemispheres within each slice to obtain slice-wise values of LC contrast for each participant.

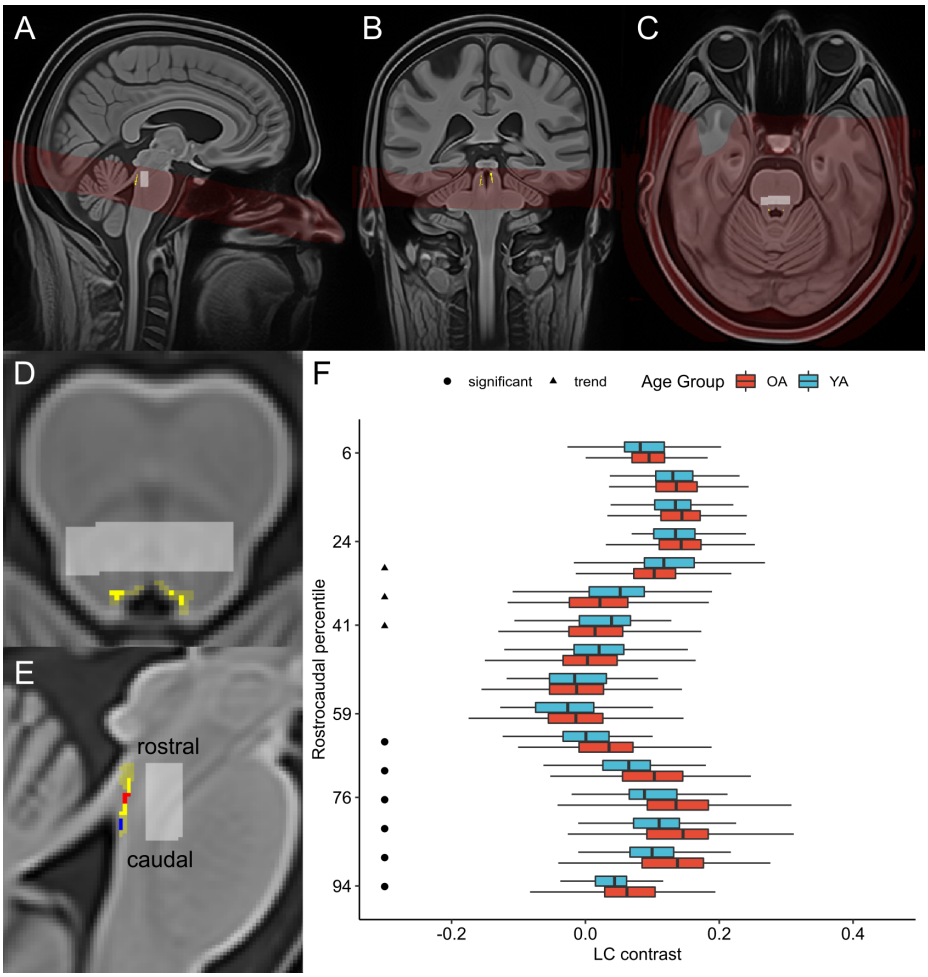

Figure 1. (A) Sagittal, (B) coronal, and (C) axial views of brainstem template volume (in red; generated from all participants' neuromelanin-sensitive scans) overlaid onto whole-brain template (generated from all participants' structural scans), with locus coeruleus (LC) probability map in common template space (Dahl et al., 2019) displayed in yellow. Pontine reference region in common template space is displayed in light gray. (D) Axial and (E) sagittal views of brainstem template volume. LC probability map (dark yellow) is overlaid onto LC search space (light yellow), both of which are shown in common template space. Pontine reference region in common template space is displayed in light gray. In (E), rostral and caudal clusters within LC probability map are depicted in red and blue, respectively. (F) Boxplots depicting LC contrast values along the LC's rostrocaudal extent are displayed for older adults (OA; red) and younger adults (YA; blue). The y-axis is arranged from most caudal (100) to most rostral (0) LC segment. For visual clarity, outliers – defined as data points falling at least 1.5 times the interquartile range below the 25% quantile or above the 75% quantile – are omitted here. A cluster-wise permutation test was performed to identify clusters of slices where contrast differed significantly by age group. Circles indicate a caudal cluster of slices where older adults had significantly greater contrast than younger adults, and triangles indicate a rostral cluster of slices where there was a trend towards older adults having lower contrast than younger adults.

2.4. Cortical Thickness Assessment

Cortical reconstruction for all T1-weighted anatomical images was performed with the Freesurfer software suite (Version 5.3.0; https://surfer.nmr.mgh.harvard.edu). Freesurfer's automated processing pipeline has been described previously and entails motion correction, brain extraction, registration to Talairach coordinates, bias field estimation and correction, and intensity normalization (Dale et al., 1999; Fischl et al., 1999). These operations were applied, and pial and white matter surfaces were generated based on intensity gradients across tissue classes. One researcher (SB) blinded to participants' age reviewed all resulting surfaces overlaid onto their respective anatomical images to identify segmentation inaccuracies that could bias subsequent thickness estimates (McCarthy et al., 2015). Only segmentation errors that did not resolve within 5 slices in any direction were manually corrected. A total of 122 (95 older adult, 27 younger adult) reconstructions contained inaccuracies on the pial surface and required that voxels be manually erased or included. This corresponded to 41.5% of older adult and 40.3% of younger adult participants' reconstructions being manually edited. The proportion of edited reconstructions did not differ by age group, $\chi^2(1, N = 296) = 0.001$, $p = .974$. For group analysis, all surfaces were tessellated and registered to a spherical atlas. Neuroanatomical labels corresponding to sulcal and gyral regions were automatically assigned to each vertex (Desikan et al., 2006; Fischl et al., 2004). At each vertex, cortical thickness was calculated as the shortest distance between the pial and white matter surfaces (Fischl & Dale, 2000). To probe relations between LC contrast and thickness of the entire cortical surface, a single, global thickness value was computed for each participant by averaging thickness over the left and right hemispheres and using the surface area of each hemisphere as a weighting factor.

2.5. Statistical Analysis

Sample characteristics of younger and older adults were compared using independent samples *t*-tests with equal variances not assumed and chi-square independence tests. Previous studies have reported age-related differences in LC contrast along the LC's rostrocaudal extent (Betts et al., 2017; Dahl et al., 2019; Liu et al., 2019; Manaye et al., 1995). To confirm that the slight sample difference in this study did not change the topographic results reported in Dahl et al. (2019), we recomputed the nonparametric,

cluster-wise permutation test using the FieldTrip toolbox (Oostenveld et al., 2011; http://www.fieldtriptoolbox.org) to identify clusters of slices where LC contrast differed significantly in younger and older adults (Maris & Oostenveld, 2007). This entailed first performing an independent samples *t*-test comparing LC contrast of older and younger adults for each slice where all subjects exhibited reliable LC signal intensity (n=16 slices). Next, clusters were formed by grouping adjacent slices where $p < 0.05$, and a cluster mass statistic for each cluster was calculated by summing the *t*-statistic values of all slices comprising each cluster. A Monte Carlo method was used to generate a permutation distribution of mass statistics for the summed *t*-statistics in each cluster under the assumption of no effect of age group on LC contrast; specifically, in each of 100,000 permutations, age group labels were shuffled, slice-wise independent samples t-tests were performed, and cluster mass statistic(s) were computed. To implement a two-tailed test, we considered a cluster significant, if its cluster mass statistic fell in the lowest or highest 2.5% of the respective permutation distribution. For each resulting cluster(s) where LC contrast differed significantly between older and younger adults, we averaged LC contrast values over the slices comprising each cluster to obtain cluster-specific LC contrast estimates for each participant.

We used multiple linear regression to determine whether LC contrast was associated with global cortical thickness and whether this association depended on age. Specifically, we constructed a regression model with overall LC contrast and chronological age as predictors of global thickness. In addition, to determine whether the effect of LC contrast on global thickness differed between older and younger adults, we included the interaction effect of overall LC contrast and age group (coded as 1=older adults, -1=younger adults) on global thickness as a predictor. Multiple linear regression analyses were subsequently conducted to examine the effects of overall LC contrast and age on global thickness in each age group separately. For ease of interpretation of results and comparison of regression coefficients across age groups, each predictor was standardized by mean centering and dividing by its standard deviation; thus, results of these analyses are reported as standardized regression coefficients and standard error values. To determine whether associations between LC contrast and thickness differed based on LC

topography, we repeated these analyses for each set of cluster-specific LC contrast values. Since we did not observe that intracranial volume scaled with global thickness in either age group, intracranial volume was not included as a predictor in the regression models.[2] In addition, exploratory analyses indicated significant sex differences in overall LC contrast and global cortical thickness, so we performed regression analyses accounting for sex and its interaction effects with other predictors on thickness (Supplementary Methods, Section 1.1). All descriptive statistics and regression analyses were performed in R (Version 3.6.2; R Core Team, 2019).

To examine locations on the cortical surface where LC contrast was associated with thickness, we fit a series of vertex-wise general linear models using Freesurfer's group analysis stream. For each age group separately, we modeled cortical thickness at each vertex as a function of overall LC contrast while regressing out the effect of chronological age. Resulting cortical maps were smoothed with a circularly symmetric Gaussian kernel of 10 mm at full width half maximum, which was chosen to balance the increase in signal-to-noise afforded by smoothing with the risk of false alarms that comes along with larger smoothing kernels. Smoothed maps were thresholded to include only vertices where $p < 0.05$. We then performed a cluster-wise correction for multiple comparisons using a Monte Carlo Null-Z simulation with 10000 iterations (Hagler et al., 2006). In each iteration, a *z*-map was generated, smoothed, and thresholded ($p < .05$), clusters were formed, and the size of the largest cluster was recorded. This resulted in a distribution of the maximum cluster size under the null hypothesis, which was then used for cluster-wise correction of the thresholded cortical maps. After clusters were identified in these maps, cluster-wise *p*-values were computed which, for each cluster, reflected the probability of a cluster with its size or larger occurring under the null hypothesis. A cluster-wise threshold of $p < 0.05$ was applied to include only those clusters unlikely to appear by chance. Results were presented as statistical maps of clusters that survived multiple comparison correction. To determine whether regionally-specific associations between

[2]We repeated all analyses of global thickness accounting for effects of intracranial volume on thickness and found only two changes to significant effects. First, the interaction effect between rostral LC contrast and age group on global thickness became significant ($\beta = 0.117$, $p = .045$). Second, the negative association between caudal LC and global thickness across the full sample became significant ($\beta = -0.162$, p = .020).

cortical thickness and LC contrast differed based on LC topography, we performed these vertex-wise analyses again using each set of cluster-specific LC contrast values. In line with analyses of global thickness, we conducted additional vertex-wise analyses accounting for sex (Supplementary Methods, Section 1.2).

3. Results

3.1. LC contrast & global cortical thickness in the sample

Overall LC contrast was comparable in younger and older adults, $t(88.6) = -1.24$, $p = .218$, and was not correlated with chronological age in either age group (Figure S1). As anticipated, global cortical thickness was significantly lower in older than in younger adults, $t(108.9) = -9.61$, $p < .001$, and was negatively correlated with age in both age groups (Figure S2). Exploratory analyses indicated significant sex differences in both overall LC contrast and global cortical thickness (Figure S3). Consistent with the findings of Dahl et al., 2019, we detected age group differences in LC contrast along the LC's rostrocaudal extent (Figure 1F). Specifically, we detected a cluster of 6 caudal slices where older adults had greater LC contrast than younger adults, $p = .002$, as well as a cluster of 3 rostral slices where there was a trend towards older adults having lower LC contrast than younger adults, $p = .083$.

3.2. Analysis of the association between LC contrast and global cortical thickness

Figure 2 depicts associations between LC contrast and cortical thickness in older and younger adults. Multiple linear regression analysis indicated that overall LC contrast and chronological age predicted 28.1% of the variance in global cortical thickness (Table 2A). In this analysis, we observed a significant interaction effect between overall LC contrast and age group on global thickness, $\beta = 0.138$, $p = .009$, indicating that the association between overall LC contrast and global thickness differed significantly in older and younger adults. We then performed multiple linear regression analyses to examine the association between overall LC contrast and global thickness for each age group separately, after regressing out effects of age on thickness. This analysis in older adults indicated that overall LC contrast and age together predicted 7.5% of the variance in global thickness (Table 2B), with higher overall LC contrast, $\beta = 0.216$, $p < .001$, and lower age, $\beta = -0.153$, $p = .018$, being significant predictors

of greater global thickness. In younger adults, neither overall LC contrast nor age was significantly associated with global thickness (Table 2C).

To examine effects of LC topography on the association between LC contrast and thickness, we performed analogous regression analyses using rostral and caudal values of LC contrast, respectively, as predictors instead of overall LC contrast. An analysis of the full sample indicated that rostral LC contrast, age, and the interaction between rostral LC contrast and age group predicted 28.6% of the variance in global thickness (Table 3A). We observed a trend towards an interaction effect between rostral LC contrast and age group, $\beta = 0.103$, $p = .082$. Although this result did not indicate a significant difference in the rostral LC contrast-global thickness association by age group, for consistency with analyses of overall LC contrast, we performed subsequent regression analyses in each age group separately. These analyses demonstrated that the rostral LC-thickness association was driven by older adults, with rostral LC contrast demonstrating a significantly positive association with global thickness in older adults, $\beta = 0.214$, $p < .001$ (Table 3B), but not in younger adults, $\beta = 0.002$, $p = .990$ (Table 3C).

A regression analysis examining the association between caudal LC contrast and global cortical thickness indicated that, across the sample, caudal LC contrast, age, and the interaction effect between caudal LC contrast and age group predicted 26.9% of the variance in global thickness (Table 4A). Across the sample, there was a trend towards caudal LC contrast being negatively associated with global thickness, $\beta = -0.128$, $p = .071$, and we also observed a marginally significant interaction effect between caudal LC contrast and age group on global thickness, $\beta = 0.135$, $p = .057$. Post-hoc regression analyses demonstrated that in older adults, caudal LC contrast was not significantly associated with global cortical thickness after accounting for effects of age, $\beta = 0.006$, $p = .922$ (Table 4B). However, in younger adults, higher caudal LC contrast significantly predicted lower global cortical thickness, $\beta = -0.241$, $p = .046$ (Table 4C). Results of supplementary analyses examining associations between LC contrast and global thickness accounting for sex are included in the Supplementary Results, Section 2.4.1.

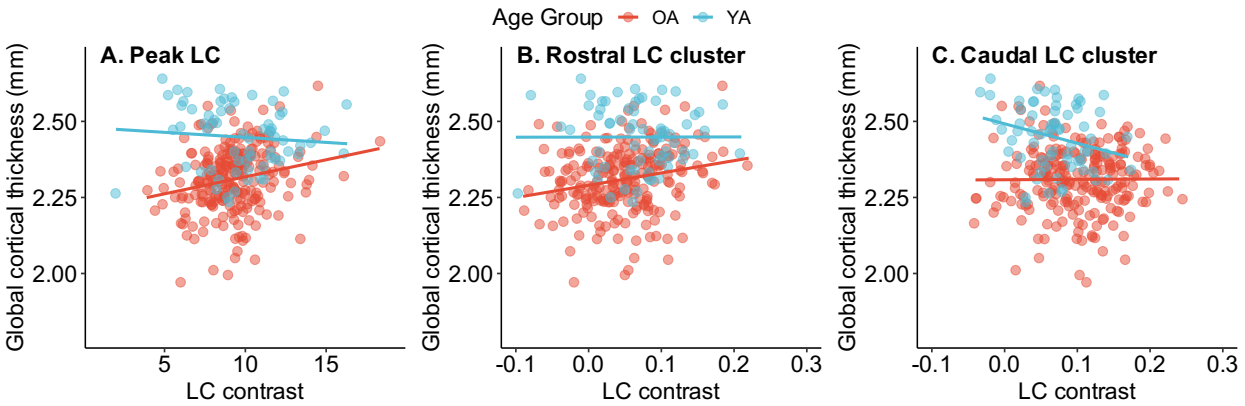

Figure 2. Associations between locus coeruleus (LC) contrast and global cortical thickness. Associations with global cortical thickness are displayed separately for older adults (OA) and younger adults (YA) for (A) overall LC contrast (reflecting contrast of peak LC voxels across x-, y-, and z-directions), (B) contrast of the rostral LC, and (C) contrast of the caudal LC. Points indicate raw data. Model fit lines reflect the association between LC contrast and global cortical thickness after regressing out the effect of chronological age on thickness. Fit lines were calculated using the mean value of chronological age within each age group.

Table 2

Results of multiple linear regression analyses examining the relationship between overall locus coeruleus contrast and global cortical thickness

Predictor	*β*	SE	95% CI	*t*	*p*
A. Full sample, $F(3, 292)=39.38$, $p<.001$, $R^2=0.288$, adjusted $R^2 = 0.281$					
Overall LC contrast	0.069	0.052	-0.033, 0.172	1.33	.185
Age	-0.506	0.050	-0.604, -0.408	-10.2	<.001
Overall LC contrast * Age Group	0.138	0.052	0.035, 0.241	2.64	.009
B. Older adults, $F(2, 226)=9.14$, $p<.001$, $R^2=0.075$, adjusted $R^2=0.067$					
Overall LC contrast	0.216	0.064	0.090, 0.342	3.37	<.001
Age	-0.153	0.064	-0.280, -0.027	-2.39	.018
C. Younger adults, $F(2, 64)=1.72$, $p=.187$, $R^2=0.051$, adjusted $R^2=0.021$					
Overall LC contrast	-0.087	0.123	-0.332, 0.158	-0.71	.482
Age	-0.198	0.123	-0.443, 0.047	-1.61	.111

Note. Regression coefficients and standard errors are standardized values. Age group was coded as: older adults = 1, younger adults = -1. CI = confidence interval; LC = locus coeruleus; SE = standard error.

Table 3

Results of multiple linear regression analyses examining the relationship between rostral locus coeruleus contrast and global cortical thickness

Predictor	*β*	SE	95% CI	*t*	*p*
A. Full sample, $F(3, 292)=38.98$, $p<.001$, $R^2=0.286$, adjusted $R^2=0.279$					
Rostral LC contrast	0.088	0.060	-0.029, 0.204	1.48	.139
Age	-0.503	0.051	-0.602, -0.403	-9.93	<.001
Rostral LC contrast * Age Group	0.103	0.059	-0.013, 0.220	1.75	.082
B. Older adults, $F(2, 226)=9.08$, $p<.001$, $R^2=0.074$, adjusted $R^2=0.066$					
Rostral LC contrast	0.214	0.064	0.088, 0.341	3.35	<.001
Age	-0.163	0.064	-0.289, -0.036	-2.54	.012
C. Younger adults, $F(2, 64)=1.46$, $p=.240$, $R^2=0.044$, adjusted $R^2=0.014$					
Rostral LC contrast	0.002	0.124	-0.246, 0.250	0.01	.990
Age	-0.209	0.124	-0.457, 0.039	-1.69	.097

Note. Regression coefficients and standard errors are standardized values. Age group was coded as: older adults = 1, younger adults = -1. CI = confidence interval; LC = locus coeruleus; SE = standard error.

Table 4

Results of multiple linear regression analyses examining the relationship between caudal LC contrast and global cortical thickness

Predictor	*β*	SE	95% CI	*t*	*p*
A. Full sample, $F(3, 292)=35.77$, $p<.001$, $R^2=0.269$, adjusted $R^2=0.261$					
Caudal LC contrast	-0.128	0.071	-0.266, 0.011	-1.81	.071
Age	-0.461	0.055	-0.570, -0.352	-8.32	<.001
Caudal LC contrast * Age Group	0.135	0.071	-0.004, 0.275	1.91	.057
B. Older adults, $F(2, 226)=3.31$, $p=.038$, $R^2=0.028$, adjusted $R^2=0.020$					
Caudal LC contrast	0.006	0.066	-0.123, 0.136	0.10	.922
Age	-0.168	0.066	-0.298, -0.039	-2.56	.011
C. Younger adults, $F(2, 64)=4.29$, $p=.018$, $R^2=0.118$, adjusted $R^2=0.091$					
Caudal LC contrast	-0.275	0.118	-0.511, -0.039	-2.33	.023
Age	-0.241	0.118	-0.477, -0.005	-2.04	.046

Note. Regression coefficients and standard errors are standardized values. Age group was coded as: older adults = 1, younger adults = -1. CI = confidence interval; LC = locus coeruleus; SE = standard error.

3.3. Analysis of the association between LC contrast and regional cortical thickness

Using vertex-wise general linear model analyses, we detected a significant association between overall LC contrast and cortical thickness in older adults in fourteen clusters on the cortical surface after regressing out the effects of chronological age on thickness. Details of the size and location of these clusters are presented in Table 5. As shown in Figure 3, these clusters included regions in frontal, parietal, occipital, and temporal cortices. In each cluster, higher overall LC contrast predicted greater cortical thickness in older adults. In younger adults, there were no clusters surviving multiple comparison correction in which overall LC contrast was associated with cortical thickness. Uncorrected maps of cortical vertices where, before multiple comparison correction, the overall LC contrast-cortical thickness relationship was significant (vertex-wise $p < 0.05$) in older and younger adults are shown in Figure S4.

Table 5

Clusters on the cortical surface where overall locus coeruleus contrast was positively associated with cortical thickness in older adults

Region	Hemi-sphere	Size (mm^2)	Peak vertex*			CWP**
			X	Y	Z	
Inferior parietal	Left	5334.79	-44.4	-70.2	9.4	0.0001
Pars triangularis	Left	2829.49	-47.9	34.8	-8.5	0.0001
Superior frontal	Left	2590.56	-8.9	2.1	67.1	0.0001
Inferior parietal	Left	1350.49	-43.3	-63.9	38.9	0.0013
Precentral	Left	1039.94	-34.7	-21	49.8	0.0102
Superior temporal	Left	910.53	-59.4	-12	-3.3	0.0244
Precentral	Right	5682.29	40.8	-10.3	58.2	0.0001
Precuneus	Right	2556.13	6.7	-57.4	32.3	0.0001
Inferior parietal	Right	2260.05	37	-53.9	38.1	0.0001
Lateral occipital	Right	1783.1	40.8	-85.3	-13	0.0001
Lingual	Right	1602.38	20.4	-74.2	-8.8	0.0002
Pars orbitalis	Right	1389.28	45.8	30.2	-12.3	0.0006
Banks of superior temporal sulcus	Right	1154.07	48.8	-40.6	12.5	0.0056
Rostral middle frontal	Right	1007.6	31	41.6	20.2	0.0138

*Talairach coordinates of vertex with peak CWP value.
**Cluster-wise probability (CWP) resulting from cluster-wise Monte Carlo correction for multiple comparisons, reflecting the probability of the cluster appearing by chance. Only clusters with CWP<.05 are listed.

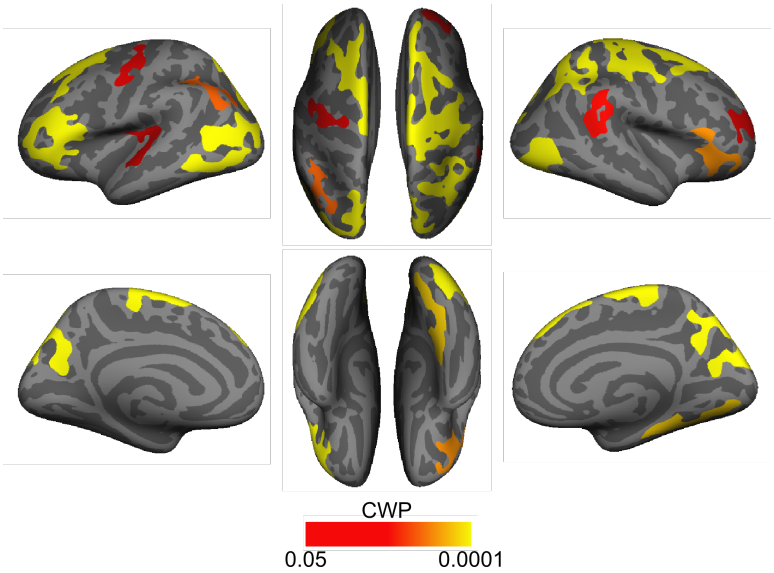

Figure 3. Cortical regions exhibiting an association between overall locus coeruleus contrast and thickness in older adults. Only clusters that survived cluster-wise correction for multiple comparisons (cluster-wise probability (CWP) < .05) are shown.

Analogous vertex-wise analyses indicated that, after correction for multiple comparisons, rostral LC contrast was positively associated with thickness in fifteen clusters on the cortical surface in older adults (Table 6A). These clusters, displayed in Figure 4A, included portions of parietal, frontal, and occipital cortices, and many overlapped with clusters where overall LC contrast was associated with thickness in older adults. In younger adults, there were no cortical clusters in which rostral LC contrast was significantly associated with thickness. In contrast, we found that caudal LC contrast was only associated with thickness in one cluster on the cortical surface in older adults (Table 6B), and in this cluster, caudal LC contrast was negatively associated with thickness. Furthermore, in younger adults, caudal LC contrast was negatively associated with thickness in three clusters on the cortical surface; these clusters included regions in parietal and occipital cortices and are described in Table S1. Figures S5 and S6 depict maps of cortical vertices where there were significant (vertex-wise $p < .05$) associations between rostral and caudal LC contrast, respectively, before cluster-wise correction for multiple comparisons. Results of supplementary, vertex-wise analyses examining associations between LC contrast and thickness accounting for sex are included in the Supplementary Results (Section 2.4.2).

Table 6

Clusters on the cortical surface where rostral (A) and caudal (B) locus coeruleus contrast were associated with cortical thickness in older adults.

Region	Hemi-sphere	Association with thickness	Size (mm^2)	Peak vertex* X	Y	Z	CWP**
A. Rostral LC contrast associated with thickness							
Pars triangularis	Left	Positive	2633.77	-48.1	35.4	-6.3	0.0001
Caudal middle frontal	Left	Positive	2288.88	-39.6	11.4	51.4	0.0001
Superior frontal	Left	Positive	1958.83	-10.1	39.7	47.9	0.0001
Superior parietal	Left	Positive	1811.48	-10.2	-87.1	29.1	0.0001
Postcentral	Left	Positive	1472.1	-47	-25.4	33.9	0.0002
Precuneus	Left	Positive	1391.17	-8.2	-45.3	44.3	0.0005
Inferior parietal	Left	Positive	1091.19	-43.3	-64.6	40.3	0.007
Precentral	Left	Positive	974.53	-45.2	-10.9	39.7	0.0166
Precentral	Right	Positive	4717.72	-39.6	11.4	51.4	0.0001
Supramarginal	Right	Positive	3809.56	-48.1	35.4	-6.3	0.0001
Lateral occipital	Right	Positive	2799.21	-8.2	-45.3	44.3	0.0001
Isthmus cingulate	Right	Positive	2070.17	-43.3	-64.6	40.3	0.0001
Rostral middle frontal	Right	Positive	1424.36	-45.2	-10.9	39.7	0.0002
Superior frontal	Right	Positive	1338.58	-47	-25.4	33.9	0.0008
Pars triangularis	Right	Positive	1096.91	-10.2	-87.1	29.1	0.0047
B. Caudal LC contrast associated with thickness							
Rostral middle frontal	Left	Negative	857.23	-19.1	57.7	-11.9	0.0351

Note. CWP = cluster-wise probability; LC = locus coeruleus.
*Talairach coordinates of vertex with peak CWP value.
**Cluster-wise probability (CWP) resulting from cluster-wise Monte Carlo correction for multiple comparisons, reflecting the probability of the cluster appearing by chance. Only clusters with CWP<.05 are listed.

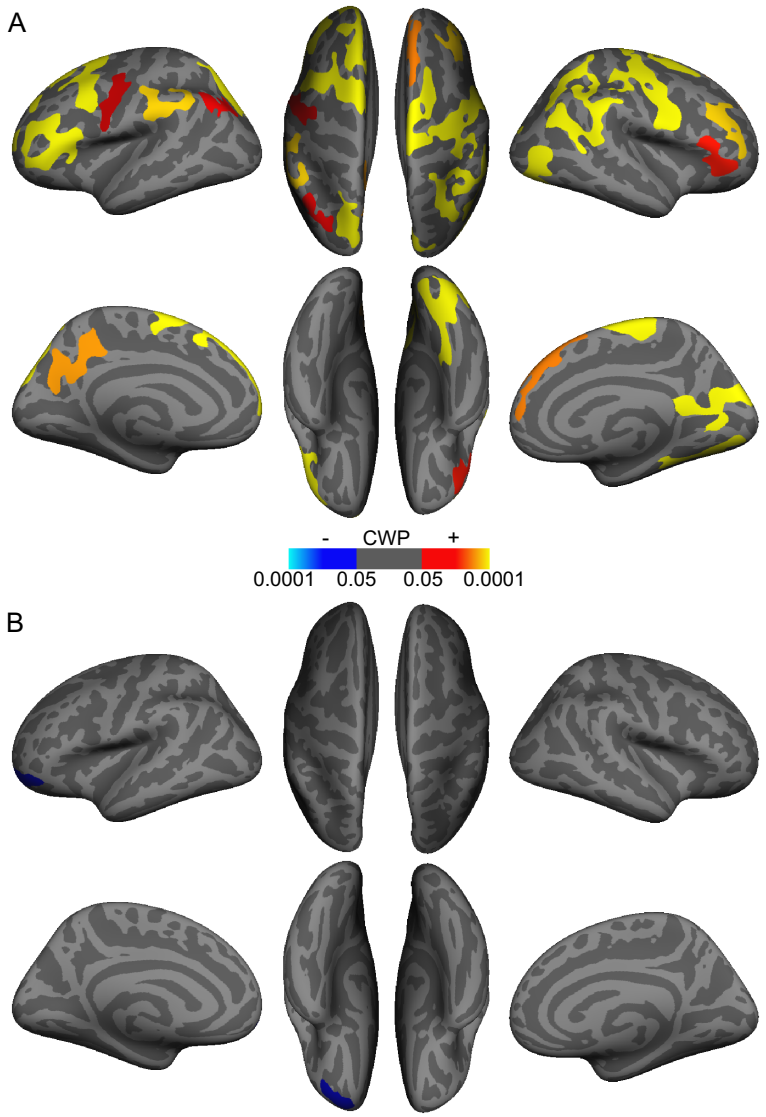

Figure 4. Cortical regions demonstrating an association between rostral (A) and caudal (B) locus coeruleus (LC) contrast and thickness in older adults. Warmer colors indicate clusters with a positive association between LC contrast and cortical thickness, and cooler colors indicate clusters with a negative association. Only clusters that survived cluster-wise correction for multiple comparisons (cluster-wise probability (CWP) <.05) are shown.

4. Discussion

A growing body of literature has suggested that the LC-NE system plays a role in cognition in later life, with recent studies linking in vivo estimates of LC neuronal integrity to cognitive outcomes in older adults (Clewett et al., 2016; Dahl et al., 2019; Hämmerer et al., 2018; Langley et al., 2020). In this study, we aimed to build upon this literature to determine whether LC neuronal integrity predicted cortical

thickness, one aspect of brain structure and a documented brain indicator of cognitive ability in older adulthood (Fjell et al., 2006; Lee et al., 2016). Using NM-sensitive MRI to estimate LC neuronal integrity in vivo as a contrast ratio, we found that in older but not in younger adults, having higher contrast of the LC was associated with greater average thickness of the cortical surface, even after regressing out effects of age on thickness. When we examined where on the cortical surface this association was most evident in older adults, we found widespread regions in parietal, frontal, and occipital cortices in which higher LC contrast was associated with greater thickness. Together, these findings constitute novel evidence for a link between LC neuronal integrity and brain structure.

What biological processes might the relationship between LC contrast and cortical thickness reflect? NE can have either protective or deleterious effects upon the whole brain. Many of its protective effects, particularly against causes of age-related neurodegeneration and neuropathology, are mediated by β-adrenergic receptors, which require higher levels of NE for activation than α-adrenergic receptors (Salgado et al., 2012). For instance, both NE and the *β*-adrenoreceptor agonist isoproterenol facilitate clearance of beta-amyloid – one marker of cognitive aging – by promoting microglial migration and phagocytosis (Heneka et al., 2010). NE also promotes anti-inflammatory responses (Feinstein et al., 2016) and the release of neurotrophic factors (Braun et al., 2014), mainly via β-adrenergic receptor activation. Finally, NE administration activates hippocampal neurogenic precursors in the process of hippocampal neurogenesis (Jhaveri et al., 2010), and this depends on β-adrenergic receptor activation (Jhaveri et al., 2014). Thus, having greater LC neuronal integrity could lead to greater levels of NE release, allowing these beneficial downstream effects of β-adrenergic receptor activation to be realized. Furthermore, Mather et al. (2016) proposed that the high levels of NE required for β-adrenergic activity can be supported by cortical 'hot spot' regions, where high glutamatergic activity stimulates even greater NE release when the LC is activated. Having greater LC integrity could help maintain the ability to stimulate these hot spots (for instance, during engaged cognitive processing), leading to further β-adrenergically-mediated protective effects. Through these processes, having relatively preserved LC integrity in older

adulthood could lead to greater protection against neuropathology and neurodegeneration to ultimately preserve brain structure.

Another clue to potentially underlying processes comes from the associations we found between LC contrast and thickness of regions in frontal, parietal, and occipital cortices. Many of the identified regions belong to sensory, association, and prefrontal cortices, all of which are innervated by the LC (Bouret & Sara, 2002; Hirschberg et al., 2017). Critically, a number of regions where thickness was associated with LC contrast are contained within the brain's frontoparietal network (FPN). The FPN constructs a modality-independent priority map of the environment (Ptak, 2012) and maintains flexible representations of internally- and externally-guided goals (Dumontheil et al., 2011; Zanto & Gazzeley, 2013). A recent study demonstrated that, in humans, frontoparietal regions show strong resting-state functional connectivity with the LC (Jacobs et al., 2018), and during arousal and attention, phasic LC activity can promote neural gain, modulating signal-to-noise ratio of neuronal activity within the FPN to direct processing toward salient and/or task-relevant stimuli (Aston-Jones & Cohen, 2005; Bouret & Sara, 2005; Corbetta et al., 2008). The FPN also provides top-down influences on visual cortex during the control of spatial attention (Hopfinger et al., 2000; Macaluso, 2010), and this link may explain why we observed associations between LC contrast and thickness in occipital brain regions.

One possibility is thus that reduced or impaired LC-NE activity later in life, resulting from reduced LC neuronal integrity, constrains cortical activity, manifesting as impairments in selective attention, memory performance, and other cognitive processes (Corbetta et al., 2008). Reduced noradrenergic signaling within brain regions implicated in NE-mediated functions, such as the FPN but also including occipital and temporal regions, could reduce NE's protective effects in these brain regions, eventually promoting gray matter atrophy. On the other hand, preserved LC integrity could maintain the NE available to act on the FPN and other brain regions and, concurrently, more of NE's protective effects being realized throughout the cortex.

In particular, a connection between LC integrity and structural integrity of the FPN offers testable hypotheses about the LC-NE system's neuroprotective role in aging. One question is whether age-related

changes in LC structure and activity relate to changes in the capacity for selective attention. One recent study demonstrated that LC activity during arousal was effective in both older and younger adults at increasing task-relevant representations; however, in the same study, arousal also increased functional connectivity between the LC and FPN less in older than in younger adults (Lee et al., 2018). In contrast, a recent study demonstrated that during rest, functional connectivity between the LC and frontoparietal brain regions was greater in older than in younger adults (Jacobs et al., 2018), raising the question of how the LC and FPN interact to dictate selective processing. Understanding the LC-FPN relationship will be an important aim for future research, as noradrenergic modulation of the FPN may have consequences for processes such as sensory perception, working memory, and episodic memory.

Our findings also point to a potentially important role of LC topography, as contrast of the rostral LC – but not the caudal LC – demonstrated associations with thickness in older adulthood. Previous work has demonstrated that cortical and thalamic projections from the LC – particularly those to frontal, sensory, and occipital cortices – tend to arise in its more rostral portion (Waterhouse et al., 1983; Waterhouse et al., 1993). Likewise, projections from the LC to the basal forebrain tend to originate more from rostral than from caudal LC (Espana & Berridge, 2006). Thus, greater rostral LC integrity could lead to more of NE's neuroprotective effects being realized in cortical regions. Supporting this idea, Dahl et al., (2019) found that rostral, but not caudal, LC contrast was associated with memory performance in older adults in a largely overlapping sample from BASE-II. Furthermore, consistent with findings of Liu et al., 2019, we found that rostral but not caudal LC exhibited age-related decline in contrast, suggesting that rostral LC may be the portion of the LC most critical for brain outcomes in older adulthood.

On the other hand, contrast of the caudal LC demonstrated markedly different associations with thickness compared to contrast of the rostral LC. Whereas in older adults caudal LC contrast was largely unrelated to thickness, it was negatively associated with thickness of the cortical surface in younger adults, particularly in parietal and occipital brain regions. As previous studies have not reported associations between cognition and integrity of the more caudal portion of the LC, we take caution in interpreting these associations. Further, NM-based MRI may be less sensitive in younger adults due to

less LC neuromelanin accumulation compared to older adults (Hämmerer et al., 2018; Mann & Yates, 1974). Nevertheless, we believe the topographical differences we observed in LC contrast – and their differential age-specific associations with cortical thickness – warrant further investigation, as over-activation of the LC in stressed younger adults may be associated with negative effects on cortical health, perhaps due to suppression of parasympathetic activity (Mather et al., 2017).

The present study has several limitations. Due to the smaller size of the younger adult cohort relative to that of the older adult cohort, results of analyses performed across the entire sample are likely driven by older adults. It is also possible that additional effects of LC contrast on thickness in younger adults would emerge with a larger younger adult sample. In addition, recent studies have identified external factors such as time of day a that may explain some portion of variability in measurements of brain structure (Karch et al., 2019), and we cannot rule out the potential influence of such factors on cortical thickness estimates in the present study. Finally, in terms of characteristics of the sample, both the younger and older adults who participated in BASE-II constituted a highly educated convenience sample (Bertram et al., 2014), meaning that results may not generalize to the general population.

We have offered hypotheses about processes underlying a relationship between LC neuronal integrity and cortical thickness, but these possibilities remain to be tested. In addition, it remains to be understood precisely what is reflected by these MRI-based measures of LC contrast. Measures of LC contrast are commonly interpreted as indices of LC neuronal integrity based on findings of Keren et al. (2015) demonstrating that locations of high NM-sensitive MRI contrast correspond to locations of NM-containing cells in the LC. One open question is whether and why having more NM is neuroprotective in older adults. One additional possibility is that the LC contrast measure reflects other features of noradrenergic neurons which also yield T1-shortening effects (e.g., water content), rather than neuromelanin (Watanabe et al., 2019a; Watanabe et al., 2019b). Furthermore, there has not yet been much work demonstrating how MRI-based LC contrast measures relate to LC function. One recent study demonstrated that LC contrast was associated with LC activity during goal-relevant processing (Clewett et al., 2018). Another recent study found that functional connectivity between LC and FPN brain regions

during an auditory oddball task was associated with LC contrast (Mather et al., 2020). However, more work is needed to understand the LC contrast-LC function relationship.

To conclude, we found that LC MRI contrast, particularly that of the rostral LC, was associated with thickness of widespread cortical regions in older but not in younger adults. These findings constitute novel evidence for a link between LC contrast and brain structure in older adulthood and are consistent with previous reports of LC contrast predicting cognition in older adulthood. Furthermore, our results provide strong motivation for studying the relationship between the LC and FPN in older adulthood, as these brain regions are implicated in attention and memory functions that undergo regular age-related decline. We believe that these findings will inform future studies of the mechanisms by which the LC-NE system protects against neuropathology and cognitive decline in aging.

Acknowledgements

Support for BASE-II was provided by the German Federal Ministry of Education and Research (Bundesministerium für Bildung and Forschung, BMBF) under grants #16SV5536 K, #16SV5537, #16SV5538, and #16SV5837, #01UW070 and #01UW0808. Additional support was provided by all six participating institutions in Germany: Max Planck Institute for Human Development, Humboldt-Universität zu Berlin, Charité-Universitätsmedizin Berlin, Max Planck Institute for Molecular Genetics, Socio-Economic Panel at the German Institute for Economic Research, Universität zu Lübeck, and Universität Tübingen. BASE-II is also part of the BMBF funded EnergI consortium (01GQ1421B).

This material is based on work supported by the National Science Foundation Graduate Research Fellowship Program under Grant No. DGE-1842487. Any opinions, findings, and conclusions or recommendations expressed in this material are those of the author(s) and do not necessarily reflect the views of the National Science Foundation. SLB's work was also supported by a Graduate Study Scholarship from the German Academic Exchange Service (DAAD). MJD was a fellow of the Max Planck Research School on the Life Course and received support from the Sonnenfeld-Foundation. MWB's work was supported by the German Research Foundation (DFG, WE 4269/5-1) and an Early Career Research Fellowship from the Jacobs Foundation. MM's work was supported by an Alexander

von Humboldt fellowship and by National Institutes of Health grant R01AG025340. We thank Michael Krause and Yana Fandakova for assistance with cluster computing, as well as Carsten Finke and Andrei Irimia for useful discussions.

Disclosure Statement

The authors have no conflicts of interest to disclose.

Data Statement

Data will be shared upon approved request to the BASE-II Steering Committee (https://www.base2.mpg.de/en/project-information/team).

References

Aston-Jones, G., Cohen, J.D., 2005. An Integrative Theory of Locus Coeruleus-Norepinephrine Function: Adaptive Gain and Optimal Performance. Annu. Rev. Neurosci. 28, 403–450. https://doi.org/10.1146/annurev.neuro.28.061604.135709

Bartrés-Faz, D., Solé-Padullés, C., Junqué, C., Rami, L., Bosch, B., Bargalló, N., Falcón, C., Sánchez-Valle, R., Molinuevo, J.L., 2009. Interactions of cognitive reserve with regional brain anatomy and brain function during a working memory task in healthy elders. Biol. Psychol. 80, 256–259. https://doi.org/10.1016/j.biopsycho.2008.10.005

Berridge, C.W., Waterhouse, B.D., 2003. The locus coeruleus-noradrenergic system: modulation of behavioral state and state-dependent cognitive processes. Brain Res. Rev. 42, 33–84. https://doi.org/https://doi.org/10.1016/S0165-0173(03)00143-7

Bertram, L., Boeckenhoff, A., Demuth, I., Duezel, S., Eckardt, R., Li, S., Lindenberger, U., Pawelec, G., Siedler, T., Wagner, G.G., Steinhagen-Thiessen, E., 2014. Cohort Profile: The Berlin Aging Study II (BASE-II). Int. J. Epidemiol. 43, 703–712. https://doi.org/10.1093/ije/dyt018

Betts, M.J., Cardenas-Blanco, A., Kanowski, M., Jessen, F., Düzel, E., 2017. In vivo MRI assessment of the human locus coeruleus along its rostrocaudal extent in young and older adults. Neuroimage 163, 150–159. https://doi.org/10.1016/j.neuroimage.2017.09.042

Betts, M.J., Cardenas-blanco, A., Kanowski, M., Spottke, A., Teipel, S.J., Kilimann, I., Jessen, F., Düzel, E., 2019a. Locus coeruleus MRI contrast is reduced in Alzheimer's disease dementia and correlates with CSF Amyloid-beta levels. Alzheimer's Dement. 11, 281–285. https://doi.org/10.1016/j.dadm.2019.02.001

Betts, M.J., Kirilina, E., Otaduy, M.C.G., Ivanov, D., Acosta-Cabronero, J., Callaghan, M.F., Lambert, C., Cardenas-Blanco, A., Pine, K., Passamonti, L., Loane, C., Keuken, M.C., Trujillo, P., Lüsebrink, F., Mattern, H., Liu, K.Y., Priovoulos, N., Fliessbach, K., Dahl, M.J., Maaß, A., Madelung, C.F., Meder, D., Ehrenberg, A.J., Speck, O., Weiskopf, N., Dolan, R., Inglis, B., Tosun, D., Morawski, M., Zucca, F.A., Siebner, H.R., Mather, M., Uludag, K., Heinsen, H., Poser, B.A., Howard, R., Zecca, L., Rowe, J.B., Grinberg, L.T., Jacobs, H.I.L., Düzel, E., Hämmerer, D., 2019b. Locus coeruleus imaging as a biomarker for noradrenergic dysfunction in neurodegenerative diseases. Brain 142, 2558–2571. https://doi.org/10.1093/brain/awz193

Bouret, S., Sara, S.J., 2002. Locus coeruleus activation modulates firing rate and temporal organization of odour-induced single-cell responses in rat piriform cortex. Eur. J. Neurosci. 16, 2371–2382. https://doi.org/10.1046/j.1460-9568.2002.02413.x

Bouret, S., Sara, S.J., 2005. Network reset: A simplified overarching theory of locus coeruleus noradrenaline function. Trends Neurosci. 28, 574–582. https://doi.org/10.1016/j.tins.2005.09.002

Braun, D., Madrigal, J.L.M., Feinstein, D.L., 2014. Noradrenergic regulation of glial activation: molecular mechanisms and therapeutic implications. Curr. Neuropharmacol. 12, 342–52. https://doi.org/10.2174/1570159X12666140828220938

Clewett, D. V, Lee, T., Greening, S., Ponzio, A., Margalit, E., Mather, M., 2016. Neuromelanin marks the spot: identifying a locus coeruleus biomarker of cognitive reserve in healthy aging. Neurobiol. Aging 37, 117–26. https://doi.org/10.1016/j.neurobiolaging.2015.09.019

Clewett, D., Huang, R., Velasco, R., Lee, T.-H., Mather, M., 2018. Locus coeruleus activity strengthens prioritized memories under arousal. J. Neurosci. 38, 2097–17. https://doi.org/10.1523/JNEUROSCI.2097-17.2017

Corbetta, M., Patel, G., Shulman, G.L., 2008. The reorienting system of the human brain: From environment to theory of mind. Neuron 58, 306–324. https://doi.org/https://doi.org/10.1016/j.neuron.2008.04.017

Dahl, M.J., Mather, M., Düzel, S., Bodammer, N.C., Lindenberger, U., Kühn, S., Werkle-Bergner, M., 2019. Rostral locus coeruleus integrity is associated with better memory performance in older adults. Nat. Hum. Behav. 3, 1203–1214. https://doi.org/10.1038/s41562-019-0715-2

Dale, A.M., Fischl, B., Sereno, M.I., 1999. Cortical surface-based analysis. I. Segmentation and surface reconstruction. Neuroimage 9, 179–94. https://doi.org/10.1006/nimg.1998.0395

Desikan, R.S., Ségonne, F., Fischl, B., Quinn, B.T., Dickerson, B.C., Blacker, D., Buckner, R.L., Dale, A.M., Maguire, R.P., Hyman, B.T., Albert, M.S., Killiany, R.J., 2006. An automated labeling system for subdividing the human cerebral cortex on MRI scans into gyral based regions of interest. Neuroimage 31, 968–80. https://doi.org/10.1016/j.neuroimage.2006.01.021

Dumontheil, I., Thompson, R., Duncan, J., 2011. Assembly and use of new task rules in fronto-parietal cortex. J. Cogn. Neurosci. 23, 168–182. https://doi.org/10.1162/jocn.2010.21439

España, R.A., Berridge, C.W., 2006. Organization of noradrenergic efferents to arousal-related basal forebrain structures. J. Comp. Neurol. 496, 668–683. https://doi.org/10.1002/cne.20946

Fedorow, H., Tribl, F., Halliday, G., Gerlach, M., Riederer, P., Double, K.L., 2005. Neuromelanin in human dopamine neurons: Comparison with peripheral melanins and relevance to Parkinson's disease. Prog. Neurobiol. 75, 109–124. https://doi.org/10.1016/j.pneurobio.2005.02.001

Feinstein, D.L., Kalinin, S., Braun, D., 2016. Causes, consequences, and cures for neuroinflammation mediated via the locus coeruleus: noradrenergic signaling system. J. Neurochem. 139, 154–178. https://doi.org/10.1111/jnc.13447

Fischl, B., Dale, A.M., 2000. Measuring the thickness of the human cerebral cortex from magnetic resonance images. Proc. Natl. Acad. Sci. U. S. A. 97, 11050–5. https://doi.org/10.1073/pnas.200033797

Fischl, B., Sereno, M.I., Dale, A.M., 1999. Cortical surface-based analysis. II: Inflation, flattening, and a surface-based coordinate system. Neuroimage 9, 195–207. https://doi.org/10.1006/nimg.1998.0396

Fischl, B., Van Der Kouwe, A., Destrieux, C., Halgren, E., Ségonne, F., Salat, D.H., Busa, E., Seidman, L.J., Goldstein, J., Kennedy, D., Caviness, V., Makris, N., Rosen, B., Dale, A.M., 2004. Automatically Parcellating the Human Cerebral Cortex. Cereb. Cortex 14, 11–22. https://doi.org/10.1093/cercor/bhg087

Fjell, A.M., Walhovd, K.B., 2010. Structural brain changes in aging: Courses, causes and cognitive consequences. Rev. Neurosci. 21, 187–221.

Fjell, A.M., Walhovd, K.B., Reinvang, I., Lundervold, A., Salat, D., Quinn, B.T., Fischl, B., Dale, A.M., 2006. Selective increase of cortical thickness in high-performing elderly--structural indices of optimal cognitive aging. Neuroimage 29, 984–94. https://doi.org/10.1016/j.neuroimage.2005.08.007

Hagler, D.J., Saygin, A.P., Sereno, M.I., 2006. Smoothing and cluster thresholding for cortical surface-based group analysis of fMRI data. Neuroimage 33, 1093–1103. https://doi.org/10.1016/j.neuroimage.2006.07.036

Hämmerer, D., Callaghan, M.F., Hopkins, A., Kosciessa, J., Betts, M., Cardenas-Blanco, A., Kanowski, M., Weiskopf, N., Dayan, P., Dolan, R.J., Düzel, E., 2018. Locus coeruleus integrity in old age is selectively related to memories linked with salient negative events. Proc. Natl. Acad. Sci. 115, 201712268. https://doi.org/10.1073/pnas.1712268115

Heneka, M.T., Nadrigny, F., Regen, T., Martinez-Hernandez, A., Dumitrescu-Ozimek, L., Terwel, D., Jardanhazi-Kurutz, D., Walter, J., Kirchhoff, F., Hanisch, U.-K., Kummer, M.P., 2010. Locus ceruleus controls Alzheimer's disease pathology by modulating microglial functions through norepinephrine. Proc. Natl. Acad. Sci. U. S. A. 107, 6058–63. https://doi.org/10.1073/pnas.0909586107

Hirschberg, S., Li, Y., Randall, A., Kremer, E.J., Pickering, A.E., 2017. Functional dichotomy in spinal- vs prefrontal-projecting locus coeruleus modules splits descending noradrenergic analgesia from ascending aversion and anxiety in rats. Elife 6. https://doi.org/10.7554/eLife.29808

Hopfinger, J.B., Buonocore, M.H., Mangun, G.R., 2000. The neural mechanisms of top-down attentional control. Nat. Neurosci. 3, 284–291. https://doi.org/10.1038/72999

Jacobs, H.I.L., Müller-Ehrenberg, L., Priovoulos, N., Roebroeck, A., 2018. Curvilinear locus coeruleus functional connectivity trajectories over the adult lifespan: a 7T MRI study. Neurobiol. Aging 69, 167–176. https://doi.org/10.1016/j.neurobiolaging.2018.05.021

Jhaveri, D.J., Mackay, E.W., Hamlin, A.S., Marathe, S. V, Nandam, L.S., Vaidya, V.A., Bartlett, P.F., 2010. Norepinephrine directly activates adult hippocampal precursors via beta3-adrenergic receptors. J. Neurosci. 30, 2795–806. https://doi.org/10.1523/JNEUROSCI.3780-09.2010

Jhaveri, D.J., Nanavaty, I., Prosper, B.W., Marathe, S., Husain, B.F.A., Kernie, S.G., Bartlett, P.F., Vaidya, V.A., 2014. Opposing effects of α2- and β-adrenergic receptor stimulation on quiescent neural precursor cell activity and adult hippocampal neurogenesis. PLoS One 9, 1–11. https://doi.org/10.1371/journal.pone.0098736

Karch, J.D., Filevich, E., Wenger, E., Lisofsky, N., Becker, M., Butler, O., Mårtensson, J., Lindenberger, U., Brandmaier, A.M., Kühn, S., 2019. Identifying predictors of within-person variance in MRI-based brain volume estimates. Neuroimage 200, 575–589. https://doi.org/10.1016/j.neuroimage.2019.05.030

Keren, N., Lozar, C.T., Harris, K.C., Morgan, P.S., Eckert, M.A., 2009. In-Vivo Mapping of the Human Locus Coeruleus. Neuroimage 47, 1261–1267. https://doi.org/10.1016/j.neuroimage.2009.06.012

Keren, N.I., Taheri, S., Vazey, E.M., Morgan, P.S., Granholm, A.-C.E., Aston-Jones, G.S., Eckert, M.A., 2015. Histologic validation of locus coeruleus MRI contrast in post-mortem tissue. Neuroimage 113, 235–45. https://doi.org/10.1016/j.neuroimage.2015.03.020

Langley, J., Hussain, S., Flores, J.J., Bennett, I.J., Hu, X., 2020. Characterization of age-related microstructural changes in locus coeruleus and substantia nigra pars compacta. Neurobiol. Aging 87, 89–97. https://doi.org/10.1016/j.neurobiolaging.2019.11.016

Lapiz, M.D.S., Morilak, D.A., 2006. Noradrenergic modulation of cognitive function in rat medial prefrontal cortex as measured by attentional set shifting capability. Neuroscience 137, 1039–1049. https://doi.org/10.1016/j.neuroscience.2005.09.031

Lee, S., Habeck, C., Razlighi, Q., Salthouse, T., Stern, Y., 2016. Selective association between cortical thickness and reference abilities in normal aging. Neuroimage 142, 293–300. https://doi.org/10.1016/j.neuroimage.2016.06.041

Lee, T.-H., Greening, S.G., Ueno, T., Clewett, D., Ponzio, A., Sakaki, M., Mather, M., 2018. Arousal increases neural gain via the locus coeruleus-norepinephrine system in younger adults but not in older adults. Nat. Hum. Behav. 2, 356–366. https://doi.org/10.1038/s41562-018-0344-1

Liu, K.Y., Acosta-Cabronero, J., Cardenas-Blanco, A., Loane, C., Berry, A.J., Betts, M.J., Kievit, R.A., Henson, R.N., Düzel, E., Howard, R., Hämmerer, D., 2019. In vivo visualization of age-related differences in the locus coeruleus. Neurobiol. Aging 74, 101–111. https://doi.org/10.1016/j.neurobiolaging.2018.10.014

Liu, K.Y., Marijatta, F., Hämmerer, D., Acosta-Cabronero, J., Düzel, E., Howard, R.J., 2017. Magnetic resonance imaging of the human locus coeruleus: A systematic review. Neurosci. Biobehav. Rev. 83, 325–355. https://doi.org/10.1016/j.neubiorev.2017.10.023

Macaluso, E., 2010. Orienting of spatial attention and the interplay between the senses. Cortex 46, 282–297. https://doi.org/10.1016/j.cortex.2009.05.010

Madrigal, J.L.M., Kalinin, S., Richardson, J.C., Feinstein, D.L., 2007. Neuroprotective actions of noradrenaline: Effects on glutathione synthesis and activation of peroxisome proliferator activated receptor delta. J. Neurochem. 103, 2092–2101. https://doi.org/10.1111/j.1471-4159.2007.04888.x

Manaye, K.F., McIntire, D.D., Mann, D.M.A., German, D.C., 1995. Locus coeruleus cell loss in the aging human brain: A non-random process. J. Comp. Neurol. 358, 79–87. https://doi.org/10.1002/cne.903580105

Mann, D.M.A., Yates, P.O., 1974. Lipoprotein pigments - Their relationship to ageing in the human nervous system. Brain 97, 489–498. https://doi.org/10.1093/brain/97.1.489

Maris, E., Oostenveld, R., 2007. Nonparametric statistical testing of EEG- and MEG-data. J. Neurosci. Methods 164, 177–190. https://doi.org/10.1016/j.jneumeth.2007.03.024

Mather, M., Clewett, D., Sakaki, M., Harley, C.W., 2016. Norepinephrine ignites local hotspots of neuronal excitation: How arousal amplifies selectivity in perception and memory. Behav. Brain Sci. 39, e200. https://doi.org/10.1017/S0140525X15000667

Mather, M., Harley, C.W., 2016. The Locus Coeruleus: Essential for Maintaining Cognitive Function and the Aging Brain. Trends Cogn. Sci. 20, 214–26. https://doi.org/10.1016/j.tics.2016.01.001

Mather, M., Huang, R., Clewett, D., Nielsen, S.E., Velasco, R., Tu, K., Han, S., Kennedy, B., 2020. Isometric exercise facilitates attention to salient events in women via the noradrenergic system. Neuroimage 116560. https://doi.org/10.1016/j.neuroimage.2020.116560

Mather, M., Joo Yoo, H., Clewett, D. V., Lee, T.-H., Greening, S.G., Ponzio, A., Min, J., Thayer, J.F., 2017. Higher locus coeruleus MRI contrast is associated with lower parasympathetic influence over heart rate variability. Neuroimage 150, 329–335. https://doi.org/10.1016/j.neuroimage.2017.02.025

McCarthy, C.S., Ramprashad, A., Thompson, C., Botti, J., Coman, I.L., Kates, W.R., 2015. A comparison of FreeSurfer-generated data with and without manual intervention. Front. Neurosci. 9, 379. https://doi.org/10.3389/fnins.2015.00379

Nyberg, L., Loevden, M., Riklund, K., Lindenberger, U., Baeckman, L., 2012. Memory aging and brain maintenance. Trends Cogn. Sci. 16. https://doi.org/10.1016/j.tics.2012.04.005

Oostenveld, R., Fries, P., Maris, E., Schoffelen, J.-M., 2011. FieldTrip: Open Source Software for Advanced Analysis of MEG, EEG, and Invasive Electrophysiological Data. Comput. Intell. Neurosci. 2011, 1–9. https://doi.org/10.1155/2011/156869

Ptak, R., 2012. The frontoparietal attention network of the human brain: Action, saliency, and a priority map of the environment. Neuroscientist 18, 502–515. https://doi.org/10.1177/1073858411409051

Robertson, I.H., 2014. A right hemisphere role in cognitive reserve. Neurobiol. Aging 35, 1375–1385. https://doi.org/10.1016/j.neurobiolaging.2013.11.028

Robertson, I.H., 2013. A noradrenergic theory of cognitive reserve: implications for Alzheimer's disease. Neurobiol. Aging 34, 298–308. https://doi.org/10.1016/j.neurobiolaging.2012.05.019

Salgado, H., Köhr, G., Trevino, M., 2012. Noradrenergic "tone" determines dichotomous control of cortical spike-timing-dependent plasticity. Sci. Rep. 2, 1–7. https://doi.org/10.1038/srep00417

Sara, S.J., 2009. The locus coeruleus and noradrenergic modulation of cognition. Nat. Rev. Neurosci. 10, 211–223. https://doi.org/10.1038/nrn2573

Sara, S.J., Bouret, S., 2012. Orienting and reorienting: the locus coeruleus mediates cognition through arousal. Neuron 76, 130–41. https://doi.org/10.1016/j.neuron.2012.09.011

Sasaki, M., Shibata, E., Tohyama, K., Takahashi, J., Otsuka, K., Tsuchiya, K., Takahashi, S., Ehara, S., Terayama, Y., Sakai, A., 2006. Neuromelanin magnetic resonance imaging of locus ceruleus and substantia nigra in Parkinson's disease. Neuroreport 17, 1215–1218. https://doi.org/10.1097/01.wnr.0000227984.84927.a7

Schwarz, L.A., Luo, L., 2015. Organization of the locus coeruleus-norepinephrine system. Curr. Biol. 25, R1051-6. https://doi.org/10.1016/j.cub.2015.09.039

Shibata, E., Sasaki, M., Tohyama, K., Kanbara, Y., Otsuka, K., Ehara, S., Sakai, A., 2006. Age-related changes in locus ceruleus on neuromelanin magnetic resonance imaging at 3 Tesla. Magn. Reson. Med. Sci. 5, 197–200. https://doi.org/10.2463/mrms.5.197

Stern, Y., 2009. Cognitive reserve. Neuropsychologia 47, 2015–2028. https://doi.org/10.1016/j.neuropsychologia.2009.03.004

Strange, B.A., Dolan, R.J., 2004. Beta-adrenergic modulation of emotional memory-evoked human amygdala and hippocampal responses. Proc. Natl. Acad. Sci. U. S. A. 101, 11454–8. https://doi.org/10.1073/pnas.0404282101

Troadec, J.D., Marien, M., Darios, F., Hartmann, A., Ruberg, M., Colpaert, F., Michel, P.P., 2001. Noradrenaline provides long-term protection to dopaminergic neurons by reducing oxidative stress. J. Neurochem. 79, 200–210. https://doi.org/10.1046/j.1471-4159.2001.00556.x

Trujillo, P., Summers, P.E., Ferrari, E., Zucca, F.A., Sturini, M., Mainardi, L.T., Cerutti, S., Smith, A.K., Smith, S.A., Zecca, L., Costa, A., 2017. Contrast mechanisms associated with neuromelanin-MRI. Magn. Reson. Med. 78, 1790–1800. https://doi.org/10.1002/mrm.26584

Watanabe, T., Tan, Z., Wang, X., Martinez-Hernandez, A., Frahm, J., 2019a. Magnetic resonance imaging of noradrenergic neurons. Brain Struct. Funct. 224, 1609–1625. https://doi.org/10.1007/s00429-019-01858-0

Watanabe, T., Wang, X., Tan, Z., Frahm, J., 2019b. Magnetic resonance imaging of brain cell water. Sci. Rep. 9, 1–14. https://doi.org/10.1038/s41598-019-41587-2

Waterhouse, B.D., Border, B., Wahl, L., Mihailoff, G.A., 1993. Topographic organization of rat locus coeruleus and dorsal raphe nuclei: Distribution of cells projecting to visual system structures. J. Comp. Neurol. 336, 345–361. https://doi.org/10.1002/cne.903360304

Waterhouse, B.D., Lin, C.S., Burne, R.A., Woodward, D.J., 1983. The distribution of neocortical projection neurons in the locus coeruleus. J. Comp. Neurol. 217, 418–431. https://doi.org/10.1002/cne.902170406

Weinshenker, D., 2018. Long road to ruin: Noradrenergic dysfunction in neurodegenerative disease. Trends Neurosci. 41, 211–223. https://doi.org/10.1016/j.tins.2018.01.010.Long

Wilson, R.S., Nag, S., Boyle, P.A., Hizel, L.P., Yu, L., Buchman, A.S., Schneider, J.A., Bennett, D.A., 2013. Neural reserve, neuronal density in the locus ceruleus, and cognitive decline. Neurology 80, 1202–8. https://doi.org/10.1212/WNL.0b013e3182897103

Zanto, T.P., Gazzaley, A., 2013. Fronto-parietal network: flexible hub of cognitive control. Trends Cogn. Sci. 17, 602–3. https://doi.org/10.1016/j.tics.2013.10.001